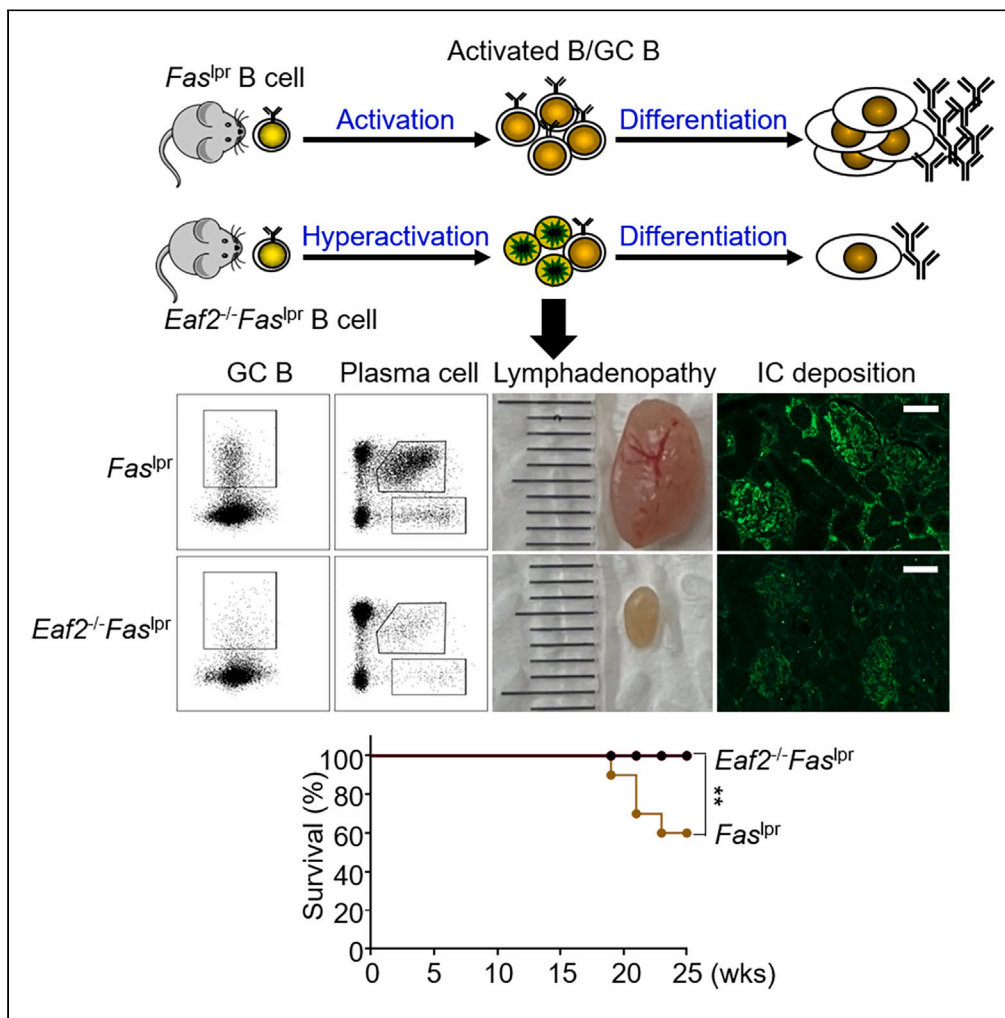


Article

EAF2 deficiency attenuates autoimmune disease in *Fas^{lpr}* mice by modulating B cell activation and apoptosis



Yingying Luan,
Qing Min, Runyun
Zhang, ..., Meiping
Yu, Lulu Dong, Ji-
Yang Wang

wang@fudan.edu.cn

Highlights

EAF2 and FAS both facilitate apoptosis in germinal center B cells

Unexpectedly, EAF2 deficiency reduces autoimmunity in *Fas^{lpr}* mice

Loss of both FAS and EAF2 leads to B cell hyperactivation and subsequent increased death

These findings underscore the complex regulation of lymphocyte apoptosis

Article

EAF2 deficiency attenuates autoimmune disease in *Fas*^{lpr} mice by modulating B cell activation and apoptosisYingying Luan,¹ Qing Min,^{2,4} Runyun Zhang,¹ Zichao Wen,¹ Xin Meng,¹ Ziyang Hu,³ Xiaoqian Feng,¹ Meiping Yu,² Lulu Dong,¹ and Ji-Yang Wang^{1,2,4,5,*}

SUMMARY

MRL/lpr mice develop systemic lupus erythematosus-like autoimmunity due to defective FAS-mediated apoptosis. We generated *Fas*^{lpr} mice deficient in EAF2, a transcription elongation-associated factor known to promote apoptosis in germinal center (GC) B cells and crucial for preventing autoimmunity. Contrary to expectations, EAF2 deficiency significantly reduced lymphadenopathy and splenomegaly, extended lifespan, and alleviated nephritis by decreasing renal immune complex deposition. Additionally, EAF2 deficiency markedly reduced accumulation of activated B cells, GC B cells, plasma cells, and the abnormal B220⁺CD3⁺ T cells in *Fas*^{lpr} mice. Further analysis revealed that *Eaf2*^{-/-} *Fas*^{lpr} B cells showed hyperactivation upon various stimulations, followed by increased death. RNA sequencing of the B220⁺CD3⁺ cells revealed a downregulation in survival-promoting genes such as *Bcl-2* and *Akt* and an upregulation of proapoptotic genes. We conclude that the combined deficiency in FAS- and EAF2-mediated apoptotic pathways leads to B cell hyperactivation and subsequent death, thereby ameliorating systemic autoimmunity in this model.

INTRODUCTION

Systemic lupus erythematosus (SLE) is a chronic autoimmune disease with significant morbidity and mortality. The disease is characterized by autoantibody production and the deposition of immune complexes, leading to multiorgan damage affecting the kidneys, skin, lungs, brain, and joints.^{1–3} In MRL/lpr mice, a classic animal model for SLE, the lymphoproliferation (lpr) mutation arises from the insertion of a 5.3 kb early transposable (ETn) element into intron 2 of the *Fas* gene. This insertion causes premature termination and aberrant splicing of the *Fas* transcript,^{4–6} leading to a defect in apoptosis. As a result, mice carrying the lpr mutation exhibit extensive lymphadenopathy and splenomegaly, elevated lymphocyte activation, autoantibody production, lupus nephritis (LN), and the accumulation of large numbers of nonmalignant B220⁺CD3⁺ T lymphocytes in lymph nodes and spleen, with LN being a primary cause of mortality.^{4,7,8}

Several immune cell lineages are abnormally activated in SLE, with B cells playing essential roles in both the onset and progression of the disease.⁹ They serve as precursors to antibody-secreting cells (ASCs), contributing to LN through autoantibody production.^{10,11} Additionally, B cells act as antigen-presenting cells (APCs) for T cell activation and produce both inflammatory and regulatory cytokines.^{12–14} However, despite the development of B cell targeted immunotherapies, including B cell activating factor inhibitors and B cell specific depleting antibodies,^{15,16} the prognosis of SLE remains poor.¹⁷ This underscores the need for a deeper understanding of the role of B cells in SLE.¹⁸

Human upregulated gene 19 (U19)/ELL-associated factor 2 (EAF2) is a potential prostate tumor suppressor¹⁹ and may also be involved in the development of acute myeloid leukemia.²⁰ As part of the super elongation complexes (SEC), EAF2 regulates transcriptional elongation through interactions with RNA polymerase II (Pol II) elongation factors known as eleven-nineteen Lys-rich leukemia (ELL) proteins.^{21–23} The SEC, comprising AF4/FMR2 (AFF) family proteins (AFF1–4), YEATS domain-containing proteins ENL or AF9 (encoded by the MLLT1 and MLLT3 genes), ELL proteins, and positive transcription elongation factor b (P-TEFb), is crucial for facilitating rapid and productive transcription by releasing RNA Pol II through its P-TEFb module and promoting transcriptional processivity with its ELL2 subunit.²⁴ Our previous work has demonstrated that EAF2 is highly expressed in germinal center (GC) B cells, where it mediates apoptosis and plays an important role in maintaining the balance between immunity and tolerance.²⁵ In the present study, we show that absence of EAF2 in *Fas*^{lpr} mice significantly alleviates LN by attenuating GC B cell expansion and plasma cell (PC) formation. Moreover, the abnormal B220⁺CD3⁺ T cells were also

¹Department of Immunology, School of Basic Medical Sciences, Fudan University, Shanghai, China

²Department of Clinical Immunology, Children's Hospital of Fudan University, National Children's Medical Center, Shanghai, China

³Department of Microbiology and Immunology, College of Basic Medical Sciences, Zhengzhou University, Zhengzhou, China

⁴Shanghai Sci-Tech Inno Center for Infection & Immunity, Shanghai, China

⁵Lead contact

*Correspondence: wang@fudan.edu.cn

<https://doi.org/10.1016/j.isci.2024.111220>



significantly reduced in *Eaf2*^{-/-}*Fas*^{lpr} mice. *In vitro* studies suggest that the dual deficiency in FAS- and EAF2-mediated apoptotic pathways leads to B cell hyperactivation followed by increased death, which contributes to the amelioration of systemic autoimmunity. These findings provide insights into the regulatory mechanisms of lymphocyte death in SLE.

RESULTS

EAF2 deficiency reduces mortality in *Fas*^{lpr} mice

To assess disease progression, we examined the body condition of mice at various ages. The body weights of wild type (WT), *Eaf2*^{-/-}, *Fas*^{lpr}, and *Eaf2*^{-/-}*Fas*^{lpr} mice showed no significant differences over time (Figure 1A). However, EAF2 deficiency significantly prolonged the survival of *Fas*^{lpr} mice (Figure 1B). This was accompanied by markedly reduced lymph node enlargement in *Eaf2*^{-/-}*Fas*^{lpr} mice (Figure 1C), particularly in the axillary (Figures 1D and 1E) and inguinal lymph nodes (Figures 1F and 1G), and diminished splenomegaly (Figures 1H and 1I).

EAF2 deficiency alleviates lupus nephritis in *Fas*^{lpr} mice

Eaf2^{-/-}*Fas*^{lpr} mice showed significant reductions in levels of IgG anti-sm/RNP (Figure 2A) and IgG anti-ANA antibodies (Figure 2B) compared to *Fas*^{lpr} mice, with no changes in IgG anti-ssDNA (Figure 2C) and anti-dsDNA (Figure 2D) antibodies. These autoantibodies form immune complexes and deposit in renal glomeruli, leading to LN,²⁶ a major cause of mortality in SLE. Histological analyses of kidney sections stained with hematoxylin and eosin (H&E) (Figure 2E) and periodic acid-Schiff (PAS) (Figure 2F) revealed significant reductions in glomerular area (Figure 2H) and cellularity (15 glomeruli analyzed randomly for each mouse) (Figure 2I) in *Eaf2*^{-/-}*Fas*^{lpr} mice. Additionally, EAF2 deficiency reduced glomerular immune complex deposition in *Fas*^{lpr} mice (Figure 2G). In agreement with the results of histological analysis, loss of EAF2 significantly lowered blood urea nitrogen (BUN) (Figure 2J) and urine protein (UP) levels (Figure 2K) in *Fas*^{lpr} mice. Collectively, these results indicate that EAF2 deficiency alleviates lupus nephritis in *Fas*^{lpr} mice.

Loss of EAF2 affects B cell development and maturation in *Fas*^{lpr} mice

B cells, crucial for SLE progression, are categorized into B-1, comprising B-1a and B-1b, and B-2, including marginal zone (MZ) and follicular (FO), B cells.²⁷ B-1a cells, part of the innate immune system, secrete natural antibodies to neutralize invading pathogens.²⁸ While *Fas*^{lpr} mice exhibited a reduction in B-1a cells, which is consistent with previous results,^{29,30} EAF2 deficiency restored their levels (Figures S2A and S2E). No significant changes were observed in B-1b cells (Figure S2F). Transitional B cells, including T2 cells, were significantly reduced (Figures S2B and S2C, S2G–S2J), while T1 cells were increased in *Eaf2*^{-/-}*Fas*^{lpr} mice (Figures S2C and S2H). In addition, the proportion of MZ B cells was restored in the absence of EAF2, with minimal impact on FO B cells (Figures S2D, S2K, and S2L).

EAF2 deficiency reduces accumulation of activated B cells, GC B cells, and plasma cells in *Fas*^{lpr} mice

Defective B cell apoptosis in *Fas*^{lpr} mice led to a marked increase in both the proportion (Figure 3A) and number (Figure 3B) of CD69⁺ B cells, which largely diminished in *Eaf2*^{-/-}*Fas*^{lpr} mice. In the GC, B cells undergo massive expansion, affinity maturation, and finally differentiate into memory B cells or plasma cells that produce high-affinity antibodies.²⁵ As shown in Figures 3C and 3D, GC B cells spontaneously accumulated in *Fas*^{lpr} mice, and loss of EAF2 markedly reduced both the proportion and number of GC B cells. *Ex vivo* apoptosis experiments conducted with annexin-V and 7-AAD staining revealed that the late (annexin-V⁺7AAD⁺) apoptotic cells were significantly reduced in *Eaf2*^{-/-} mice and *Fas*^{lpr} mice compared to WT mice (Figures 3E and 3F), consistent with the notion that both EAF2 and FAS mediate GC B cell apoptosis. Remarkably, *Eaf2*^{-/-}*Fas*^{lpr} GC B cells exhibited elevated proportions of the late apoptotic populations compared to *Fas*^{lpr} GC B cells (Figures 3E and 3F), suggesting that the dual loss of EAF2 and FAS resulted in increased death of GC B cells. *Fas*^{lpr} mice also contained a high proportion and absolute number of B220⁺CD138⁺ plasmablasts (Figures 3G and 3H) and B220⁺CD138⁺ plasma cells (Figures 3G and 3I) in the spleen, which were significantly reduced in the absence of EAF2. Consistent with these findings, EAF2 deficiency resulted in greatly reduced levels of total immunoglobulin M (IgM), IgA, and IgG antibodies (Figures 3J–3L).

EAF2 deficiency reduces excessive PC formation in *Fas*^{lpr} B cells by inducing cell death

To investigate whether the accumulation of plasma cells in *Fas*^{lpr} mice (Figures 3G–3L) is due to an intrinsic abnormality in B cells, we isolated naive B cells and induced their PC differentiation *in vitro* with either CD40L + IL4 + IL21 (CII) or LPS stimulation for 72 h. The purity of B cells was >90% as revealed by their B220 and CD3 expression (Figure S3A), with <1% of abnormal B220⁺CD3⁺ cells, <1% of B220⁺CD138⁺ PB, and <3% of GL7⁺ GC B cells (Figures S3A–S3C). In line with the *in vivo* data, *Fas*^{lpr} B cells generated a higher proportion of the B220⁺CD138⁺ plasmablasts than WT B cells under both CLL and LPS stimuli (Figures 4A, 4B, 4G, and 4H), which were significantly reduced in the absence of EAF2. ELISPOT enumeration also confirmed fewer IgM and IgG secreting cells in *Eaf2*^{-/-}*Fas*^{lpr} mice (Figures 4C–4F; 4I–4L).

To understand the mechanism behind the decreased PC formation in *Eaf2*^{-/-}*Fas*^{lpr} B cells, we examined B cell activation and death during their PC differentiation *in vitro*. After 24 h of CII and LPS stimulation, B cells from *Eaf2*^{-/-}*Fas*^{lpr} mice displayed significantly higher levels of CD86 expression (Figure 4M), increased cell size (Figure 4N), and reduced cell death (Figures 4O and S4B), indicating higher cellular activation compared to *Fas*^{lpr} mice. Similar results were obtained when *Eaf2*^{-/-}*Fas*^{lpr} B cells were stimulated with F(ab)₂-anti-IgM antibodies, CD40L and IL4 (ACI) (Figure S4A). The increased cell size persisted even after 72 h of either CII or LPS stimulation (Figure 4P). However, these hyperactivated *Eaf2*^{-/-}*Fas*^{lpr} B cells exhibited elevated death compared to *Fas*^{lpr} B cells after 72 h of stimulation (Figure 4Q and S4B).

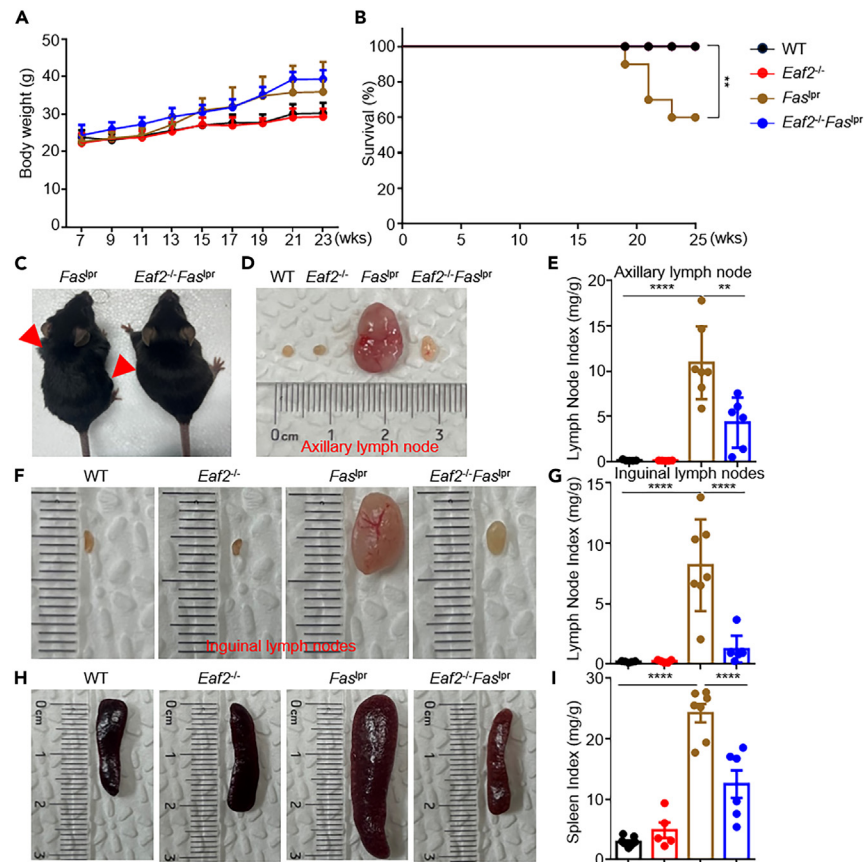


Figure 1. EAF2 deficiency reduces mortality in Fas^{lp} mice

WT, $Eaf2^{-/-}$, Fas^{lp} , and $Eaf2^{-/-}Fas^{lp}$ female mice were evaluated, with all mice sacrificed at 25 weeks ($n \geq 3$).

(A) Body weight monitored from ages 7 to 23 weeks.

(B) Survival curves. We included 12 WT, 12 $Eaf2^{-/-}$, 10 Fas^{lp} , and 12 $Eaf2^{-/-}Fas^{lp}$ female mice in the survival analysis. $**p < 0.01$ (Log rank test).

(C) Appearance of Fas^{lp} and $Eaf2^{-/-}Fas^{lp}$ female mice.

(D–G) (D and E) Axillary and (F and G) inguinal lymph node sizes.

(H and I) Spleen size. Lymph node and spleen weight index is expressed as mg/g body weight. Results from three or more independent experiments are shown as mean \pm SEM. $**p < 0.01$; $****p < 0.0001$ (one-way ANOVA).

Carboxyfluorescein succinimide ester (CFSE) *in vitro* proliferation assays indicated that EAF2 deficiency did not affect B cell proliferation (Figure S4C). We hypothesize that the excessive activation of $Eaf2^{-/-}Fas^{lp}$ B cells, as revealed by increased CD86 expression and significantly enlarged cell size, is followed by increased death, consequently reducing PC generation.

EAF2 deficiency reduces abnormal $B220^{+}CD3^{+}$ and $CD4^{-}CD8^{-}$ double-negative T cells in Fas^{lp} mice through enhanced apoptosis

The splenomegaly and lymphadenopathy in Fas^{lp} mice are associated with the accumulation of aberrant $B220^{+}CD3^{+}$ T cells, the majority of which were $CD4^{-}CD8^{-}$ double-negative (DN) T cells. These $B220^{+}CD3^{+}$ DN T cells contribute to autoimmunity by producing pro-inflammatory cytokines, inducing GC formation, promoting autoantibody production, and contributing to organ damage.^{31–33} Notably, the $B220^{+}CD3^{+}$ cells were significantly reduced in $Eaf2^{-/-}Fas^{lp}$ mice compared to Fas^{lp} mice (Figures 5A and 5B). To determine why the abnormal T cells accumulate in Fas^{lp} mice, we examined the apoptosis of these $B220^{+}CD3^{+}$ cells using flow cytometry, employing annexin-V and 7-AAD staining. In Fas^{lp} mice, there was a marked decrease in the annexin-V⁺7-AAD⁺ cells, which was significantly increased in $Eaf2^{-/-}Fas^{lp}$ mice (Figures 5C and 5D). Within the $B220^{+}CD3^{+}$ cells, the proportion of the DN T cells was further reduced in $Eaf2^{-/-}Fas^{lp}$ mice (Figures 5E and 5F). This reduction was associated with an increase in apoptosis (Figures 5G and 5H), indicating that EAF2 and FAS double deficiency enhanced apoptosis in the DN T population. However, EAF2 deficiency in Fas^{lp} mice had little effect on the proliferation of these abnormal T cells, as measured by Ki-67 expression (Figure S5), suggesting that apoptosis, rather than proliferation, regulates these cells.

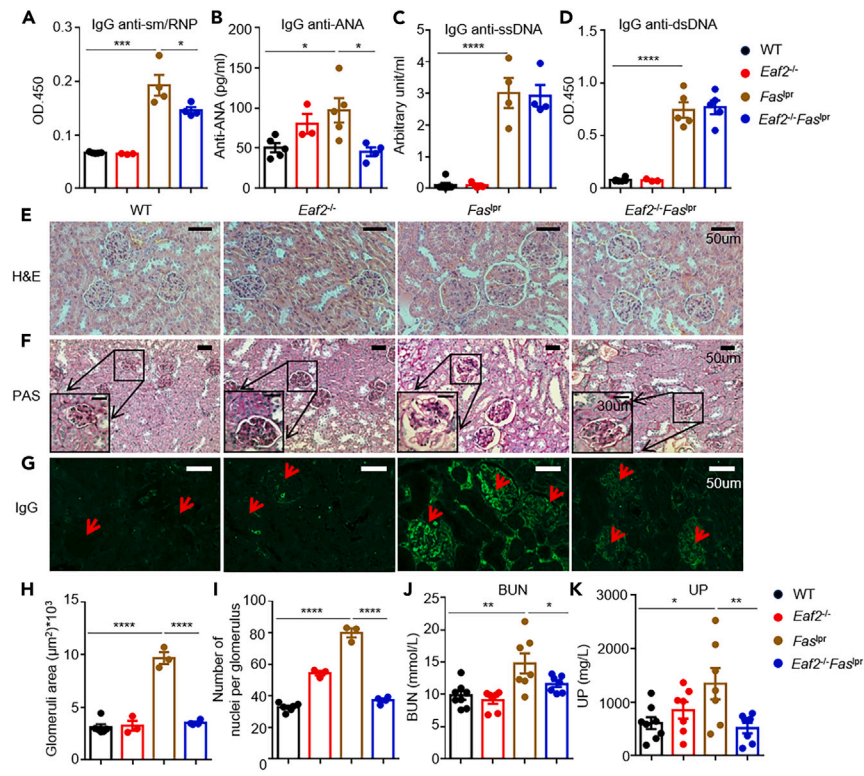


Figure 2. EAF2 deficiency alleviates lupus nephritis in *Fas*^{Lpr} mice

(A–D) WT, *Eaf2*^{-/-}, *Fas*^{Lpr}, and *Eaf2*^{-/-}*Fas*^{Lpr} female mice at 17 weeks were evaluated for levels of IgG anti-sm/RNP (A), IgG anti-ANA (B), IgG anti-ssDNA (C), and IgG anti-dsDNA autoantibodies (D).

(E–G) Kidney damage evaluated at age 25 weeks (E) H&E staining of kidney sections. Scale bar: 50 μm. (F) PAS staining. Scale bar: 50 μm and 30 μm (inset). (G) IgG immune complex deposition, indicated by red arrows. Scale bar, 50 μm.

(H) Glomerular area and (I) Glomerular cell numbers.

(J and K) Levels of BUN and UP. Data analyzed using one-way ANOVA or one-tailed unpaired Student's t test. **p* < 0.05; ***p* < 0.01; ****p* < 0.001; *****p* < 0.0001. Results presented as mean ± SEM.

EAF2 deletion promotes apoptosis in B220⁺CD3⁺ cells: Evidence from RNA-seq analysis

To delineate the signaling pathways involved in apoptosis, we sorted B220⁺CD3⁺ cells from *Fas*^{Lpr} and *Eaf2*^{-/-}*Fas*^{Lpr} mice for RNA sequencing (RNA-seq) analysis. As expected, EAF2 expression was low in the abnormal T cells from *Eaf2*^{-/-}*Fas*^{Lpr} mice compared with those from *Fas*^{Lpr} mice (Figure 6A). RNA-seq data identified 196 genes significantly down-regulated and 592 genes up-regulated in *Eaf2*^{-/-}*Fas*^{Lpr} mice compared with *Fas*^{Lpr} group. (Q value ≤ 0.05; Log₂FC ≥ 1) (Figure 6B). Gene Set Enrichment Analysis (GSEA) (Figure 6C) and Kyoto Encyclopedia of Genes and Genomes (KEGG) analysis (Figure 6D) highlighted significant enrichment in genes associated with apoptosis and those in the MAPK, TNF, and NF-κB signaling pathways in EAF2-deficient B220⁺CD3⁺ cells. Visualizations including a volcano plot (Figure 6E), heatmap (Figure 6F), and violin plot (Figure 6G) highlighted multiple enrichment terms emphasizing changes in both anti-apoptosis and pro-apoptosis genes. Notably, levels of anti-apoptosis genes (Figure 6G) *Bcl-2* and phosphorylated-protein kinase B (*Akt*) were decreased in the B220⁺CD3⁺ cells of *Eaf2*^{-/-}*Fas*^{Lpr} mice, while transcription levels of pro-apoptosis genes (Figure 6H), such as *Atf4*, *Jun*, and *Fos* were increased. These findings underscore the role of EAF2 deficiency in promoting apoptosis within this specific T cell subset.

DISCUSSION

Our previous work established that EAF2 mediates apoptosis in GC B cells, playing a crucial role in preventing excessive B cell activation and autoimmunity. Notably, the present study demonstrates that EAF2 deficiency actually ameliorates, rather than exacerbates, systemic autoimmunity in *Fas*^{Lpr} mice. This presents a paradox where the loss of two apoptotic pathways results in an unexpected reversal of the anticipated phenotype, underscoring the complex interplay within the immune system.

Fas^{Lpr} mice characteristically display immunological abnormalities including the accumulation of activated B cells, GC B cells, PC cells, and abnormal B220⁺CD3⁺ T cells, along with splenomegaly and lymph adenopathy. Remarkably, EAF2 deficiency reversed all these aberrant phenotypes, including the reduction of B220⁺CD3⁺ T cells, despite EAF2 primarily being expressed in GC B cells among the immune cells. This finding is consistent with prior studies that have highlighted the central role of B cells in lymphoproliferation observed in *Fas*^{Lpr} mice.^{34–36} FAS

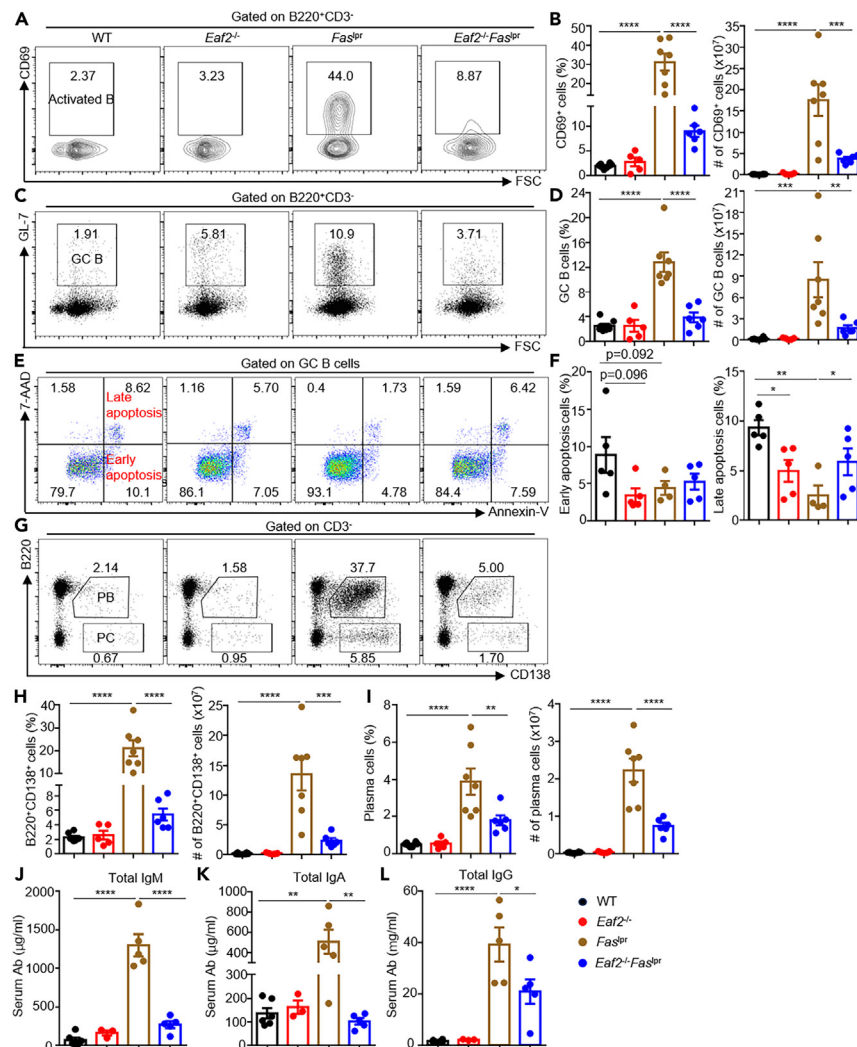


Figure 3. EAF2 deficiency reduces accumulation of activated B cells, GC B cells, and plasma cells in *Fas*^{Lpr} mice

(A–D) Flow cytometry analysis of B cell activation (A and B) and GC B cell expansion (C and D).

(E and F) Proportion of apoptotic cells among GC B cells.

(G–I) Proportions and absolute numbers of PB and PC.

(J–L) Levels of total IgM, IgG, and IgA antibodies measured by ELISA. Data expressed as mean ± SEM, with statistical significance determined by one-way ANOVA and paired t test. **p* < 0.05; ***p* < 0.01; ****p* < 0.001; *****p* < 0.0001.

expression in GC B cells has been shown to be crucial for maintaining T and B cell homeostasis.³⁷ Thus, by promoting B cell apoptosis, EAF2 deficiency significantly mitigated the immune dysregulation in *Fas*^{Lpr} mice.

LN is by far the major determinant of long-term prognosis and mortality in patients with SLE due to its serious complications.^{38,39} Similarly, *Fas*^{Lpr} mice develop LN, resulting in a significantly shortened lifespan.^{40,41} Our findings show that the absence of EAF2 extended lifespan in these mice, accompanied by decreased autoantibody production, reduced immune complex deposition in the kidneys, and attenuated LN, as revealed by improved histology of glomeruli and significantly lower UP levels. Thus, EAF2 deficiency not only reverses all aberrant immune phenotypes but also substantially alleviates the lethal nephritis in *Fas*^{Lpr} mice.

Activation-induced cell death (AICD) generally follows lymphocyte activation and is primarily mediated by FAS-FAS ligand interaction.^{42,43} Our data suggest that EAF2 deficiency leads to hyperactivation of *Fas*^{Lpr} lymphocytes, which is followed by increased cell death. This is evidenced by a significant reduction in both the proportion and total number of GC B cells in *Eaf2*^{-/-}*Fas*^{Lpr} mice compared to *Fas*^{Lpr} controls, along with increased apoptosis. Further *in vitro* experiments showed that *Eaf2*^{-/-}*Fas*^{Lpr} B cells expressed significantly higher levels of CD86 after 24 h of stimulation with either LPS, CD40L + IL4 + IL21 or α-IgM + CD40L + IL4, compared to *Fas*^{Lpr} B cells. Notably, these hyperactivated cells subsequently experienced increased cell death. RNA-seq analysis also showed elevated expression of pro-apoptotic genes and a reduction in anti-apoptotic genes in the abnormal B220⁺CD3⁺ T cells from *Eaf2*^{-/-}*Fas*^{Lpr} mice. These observations collectively suggest that the

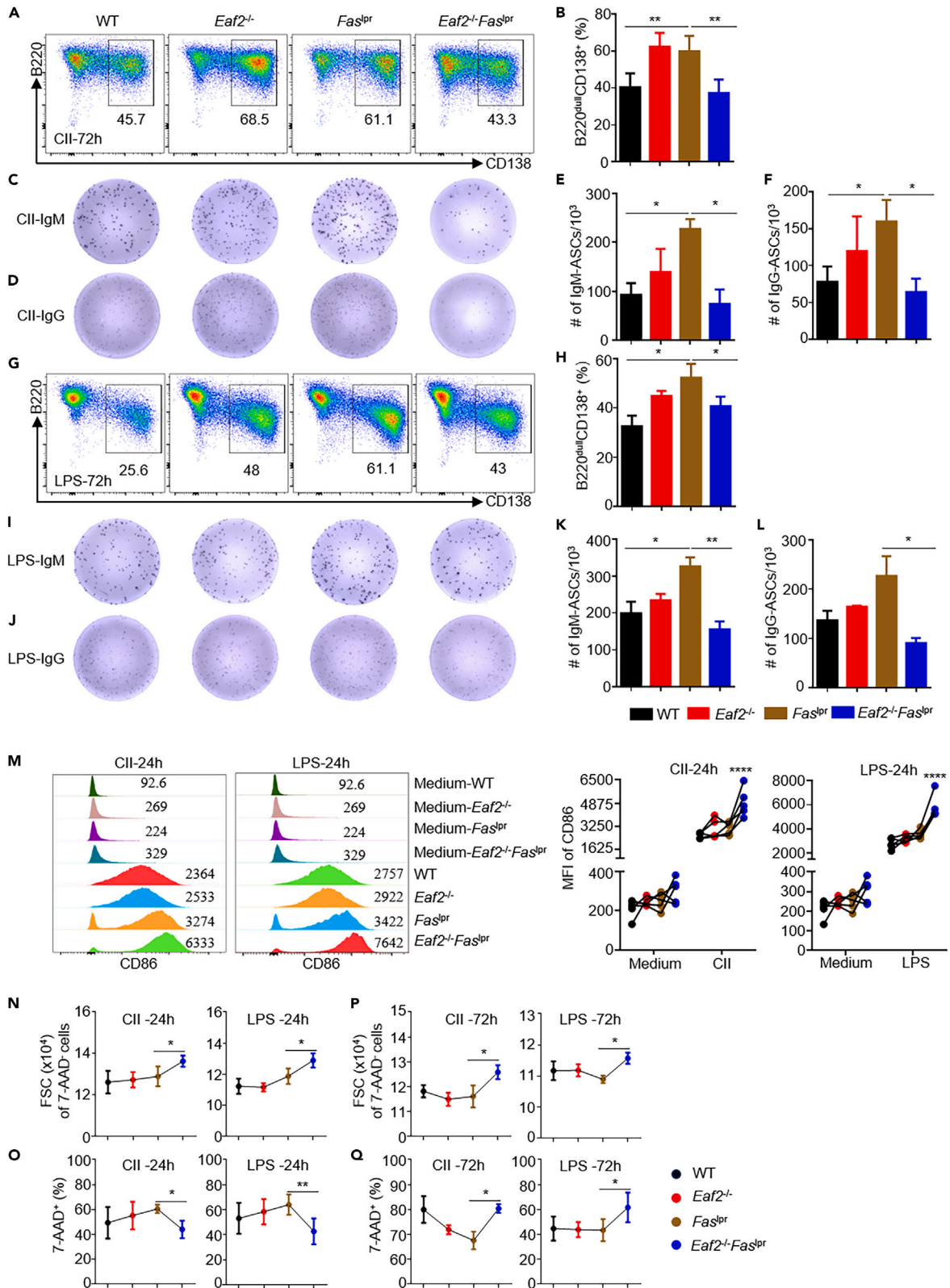


Figure 4. Absence of EAF2 reduces excessive PC generation in *Fas*^{lpr} B cells by inducing cell death

Purified naive B cells from WT, *Eaf2*^{-/-}, *Fas*^{lpr}, *Eaf2*^{-/-}*Fas*^{lpr} female mice were induced to differentiate into PC *in vitro* with CII and LPS stimulation for 72 h (n ≥ 3). (A) Representative flow cytometry plots showing PC populations (B220^{low/-}CD138⁺) after CII stimulation for 72 h. (B) Summary of results from 5 independent experiments, analyzing 5 mice from each genotype (WT, *Eaf2*^{-/-}, *Fas*^{lpr}, and *Eaf2*^{-/-}*Fas*^{lpr}). (C–F) ELISPOT analysis of IgM (C and E) and IgG (D and F) plasma cells after CII stimulation. (G and H) Proportions of PC after LPS stimulation. (I–L) ELISPOT analysis for IgM (I and K) and IgG (J and L) plasma cells. (M) CD86 expression in B cells after 24 h stimulation with CII or LPS. (N–Q) Forward scatter (FSC) of live B cells and cell death after 24 h (N and O) or 72 h (P and Q) stimulation with CII or LPS. Data expressed as mean ± SEM. *p < 0.05; **p < 0.01; ****p < 0.0001 (M, two-way ANOVA; E, F, K, and L, two-tailed unpaired Student’s t test; B, H, N–Q, paired t test).

concurrent deficiency of FAS and EAF2 apoptotic pathways does not merely exacerbate the expected phenotype but can lead to an opposite outcome. This outcome may resemble AICD but is not mediated by the traditional FAS-FASL system. One hypothesis is that the excessive activation and proliferation observed in *Eaf2*^{-/-}*Fas*^{lpr} B cells may not be sustainable due to insufficient nutrition supply. It is also conceivable that the absence of both FAS and EAF2 pathways sensitizes or activates alternative cell death pathways by allowing them to utilize effector molecules typically engaged by FAS- or EAF2-triggered signals. Since the experiments were performed on F2 mice with a mixed B6 and MRL genetic background, we cannot rule out the possibility that a gene derived from B6, which may limit autoimmunity, is closely linked to the *Eaf2* allele. Further studies are required to explore how the dual absence of these apoptotic pathways induces cell death. Understanding this cell death mechanism could provide valuable insights into developing alternative therapeutic strategies for lymphoproliferation disorders, such as autoimmune lymphoproliferative syndrome (ALPS), which is caused by FAS mutations, and other disorders associated with immune dysregulation and lymphocyte accumulation.

SLE is a chronic autoimmune disease predominantly affecting women, especially those of childbearing age,⁴⁴ presenting with a spectrum of symptoms ranging from mild arthralgias and rash to more severe nephropathy, hematological abnormalities and neuropsychiatric involvement.⁴⁵ Despite advances in understanding the mechanisms contributing to SLE, treatment options remain limited. Given the high expression of EAF2 in human B cells and Burkitt’s lymphomas (Figure S6), the potential impact of targeting EAF2 on SLE pathogenesis and B lymphomas remains to be investigated.

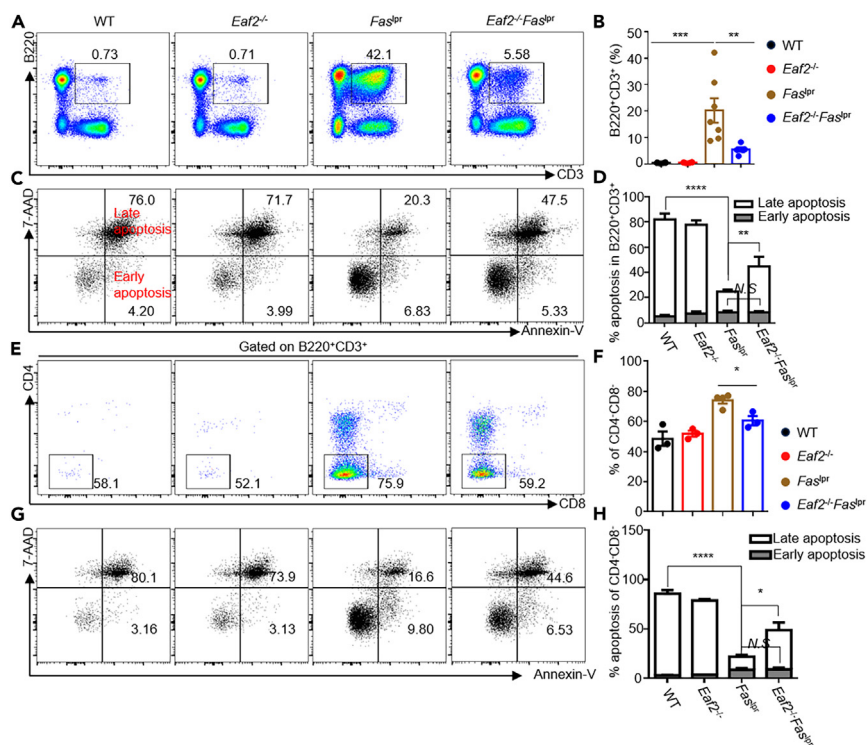


Figure 5. EAF2 deficiency reduces abnormal B220⁺CD3⁺ T cells in *Fas*^{lpr} mice through enhanced apoptosis

(A–D) Frequency of the abnormal B220⁺CD3⁺ cells (A and B) and apoptotic cells (C and D) in WT, *Eaf2*^{-/-}, *Fas*^{lpr}, and *Eaf2*^{-/-}*Fas*^{lpr} female mice (7–12 weeks, n ≥ 3). (E–H) Proportions of B220⁺CD3⁺ DN T cells (E and F) and apoptotic cells (G and H). Data in B and D are shown as mean ± SEM, with statistical significance analyzed by one-way or two-way ANOVA. *p < 0.05; **p < 0.01; ***p < 0.001; ****p < 0.0001.

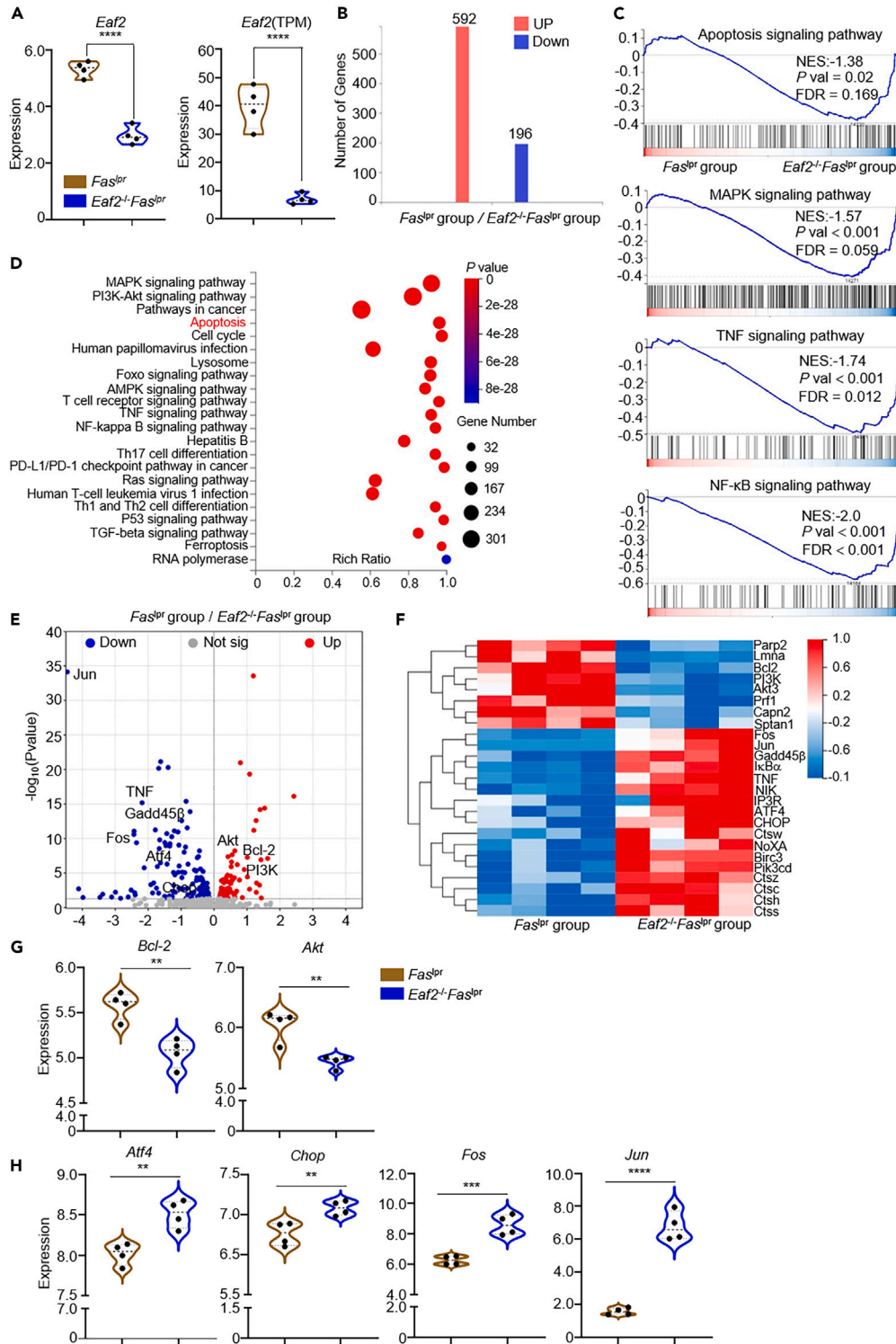


Figure 6. EAF2 deletion promotes apoptosis in B220⁺CD3⁺ cells: evidence by RNA-Sequence

B220⁺CD3⁺ cells were sorted from *Fas*^{flp} and *Eaf2*^{-/-}*Fas*^{flp} female mice aged 7–12 weeks (n = 4).

(A) *Eaf2* expression in B220⁺CD3⁺ cells from *Fas*^{flp} and *Eaf2*^{-/-}*Fas*^{flp} mice. Left, Log₂(TPM+1); right, TPM.

(B) Differentially expressed genes (DEGs) between the B220⁺CD3⁺ cells from *Fas*^{flp} and *Eaf2*^{-/-}*Fas*^{flp} mice.

(C) Gene Set Enrichment Analysis (GSEA).

(D) KEGG bubble chart.

Figure 6. Continued

(E) Volcano plot.

(F) Heatmap.

(G) Expression of anti-apoptosis genes *Bcl-2* and *Akt*.

(H) Expression of pro-apoptosis genes *Atf4*, *Chop*, *Fos*, and *Jun*. Statistics calculated by two-tailed unpaired Student's t test, **p < 0.01; ***p < 0.001; ****p < 0.0001.

In summary, EAF2 deficiency in *Fas*^{lpr} mice led to an amelioration, rather than exacerbation, of systemic autoimmunity. Further investigation revealed that *Eaf2*^{-/-}*Fas*^{lpr} B cells become hyperactivated upon stimulation, followed by elevated cell death. These observations underscore the complexity of the gene regulatory network in activated lymphocytes and suggest a potentially alternative approach for alleviating systemic autoimmunity caused by FAS deficiency.

Limitations of the study

This study was performed using mice with a mixed B6 and MRL genetic background. Consequently, it is possible that a gene from the B6 lineage, which may suppress autoimmunity, is closely linked to the *Eaf2* allele, potentially influencing the results. Additionally, while our results indicate that *Eaf2*^{-/-}*Fas*^{lpr} B cells are hyperactivated upon stimulation, followed by elevated cell death, the specific mechanisms that trigger alternative apoptosis pathways have not been fully elucidated and warrant further investigation.

RESOURCE AVAILABILITY**Lead contact**

Requests for resources and reagents should be directed to and will be fulfilled by the lead contact, Ji-Yang Wang (wang@fudan.edu.cn).

Materials availability

All materials described in this study are available from the [lead contact](#) upon request.

Data and code availability

- **Data:** RNA-seq data have been deposited at NCBI and are publicly available as of the date of publication. Accession number is listed in the [key resources table](#).
- **Code:** This paper does not report the original code.
- **Additional information:** Any additional information reported in the paper will be shared by the [lead contact](#) upon request.

ACKNOWLEDGMENTS

We thank the members in Wang laboratory for their helpful discussions. This work was supported by the Major Research Plan of the National Natural Science Foundation of China (grant #32330033 to J.-Y.W.), the National Natural Science Foundation of China (grant #32270932 to J.-Y.W.), National Natural Science Foundation for Young Scholar (grant #82202013 to Q.M. and #82402110 to X.M.), and China Postdoctoral Science Foundation Grant (grant #2022M720782 to Q.M.).

AUTHOR CONTRIBUTIONS

Y.L. conducted most experiments and drafted the manuscript; Y.L. and Q.M. designed the experiments; R.Z. handled mouse breeding and genotyping; Z.W. assisted with flow cytometry; X.M. supervised the study; Z.H., X.F., M.Y., and L.D. analyzed data. J.-Y.W. designed the study, secured funding, and finalized the manuscript.

DECLARATION OF INTERESTS

The authors declare no competing interests.

STAR★METHODS

Detailed methods are provided in the online version of this paper and include the following:

- [KEY RESOURCES TABLE](#)
- [EXPERIMENTAL MODEL AND STUDY PARTICIPANT DETAILS](#)
 - Mouse model
- [METHOD DETAILS](#)
 - Evaluation of renal injury
 - ELISA
 - Flow cytometry
 - Apoptosis assay
 - B cell purification and ex vivo stimulation
 - ELISPOT assay
 - RNA sequencing (RNA-seq)
- [QUANTIFICATION AND STATISTICAL ANALYSIS](#)

SUPPLEMENTAL INFORMATION

Supplemental information can be found online at <https://doi.org/10.1016/j.isci.2024.111220>.

Received: July 15, 2024

Revised: October 6, 2024

Accepted: October 17, 2024

Published: October 21, 2024

REFERENCES

- Pan, L., Lu, M.P., Wang, J.H., Xu, M., and Yang, S.R. (2020). Immunological pathogenesis and treatment of systemic lupus erythematosus. *World J. Pediatr.* 16, 19–30. <https://www.ncbi.nlm.nih.gov/pubmed/30796732>.
- Wu, Y., He, S., Bai, B., Zhang, L., Xue, L., Lin, Z., Yang, X., Zhu, F., He, P., Tang, W., and Zuo, J. (2016). Therapeutic effects of the artemisinin analog SM934 on lupus-prone MRL/lpr mice via inhibition of TLR-triggered B-cell activation and plasma cell formation. *Cell. Mol. Immunol.* 13, 379–390. <https://www.ncbi.nlm.nih.gov/pubmed/25942599>.
- Zhang, Q., Xiang, L., Zaman, M.H., Dong, W., He, G., and Deng, G.M. (2019). Predominant Role of Immunoglobulin G in the Pathogenesis of Splenomegaly in Murine Lupus. *Front. Immunol.* 10, 3020. <https://www.ncbi.nlm.nih.gov/pubmed/32082297>.
- Adachi, M., Watanabe-Fukunaga, R., and Nagata, S. (1993). Aberrant transcription caused by the insertion of an early transposable element in an intron of the Fas antigen gene of lpr mice. *Proc. Natl. Acad. Sci. USA* 90, 1756–1760. <https://www.ncbi.nlm.nih.gov/pubmed/7680478>.
- Mountz, J.D., Zhou, T., Bluethmann, H., Wu, J., and Edwards, C.K., 3rd (1994). Apoptosis defects analyzed in TcR transgenic and fas transgenic lpr mice. *Int. Rev. Immunol.* 11, 321–342. <https://www.ncbi.nlm.nih.gov/pubmed/7528763>.
- Wu, J., Zhou, T., Zhang, J., He, J., Gause, W.C., and Mountz, J.D. (1994). Correction of accelerated autoimmune disease by early replacement of the mutated lpr gene with the normal Fas apoptosis gene in the T cells of transgenic MRL-lpr/lpr mice. *Proceedings of the National Academy of Sciences* 91, 2344–2348. <https://www.ncbi.nlm.nih.gov/pubmed/7510888>.
- Xiang, L., Liu, A., and Xu, G. (2020). Expression of XBP1s in B lymphocytes is critical for pristane-induced lupus nephritis in mice. *Am. J. Physiol. Ren. Physiol.* 318, F1258–F1270. <https://www.ncbi.nlm.nih.gov/pubmed/32249615>.
- Zheng, X., Dozmorov, M.G., Strohle, C.E., Bastacky, S., and Sawalha, A.H. (2023). Ezh2 Knockout in B Cells Impairs Plasmablast Differentiation and Ameliorates Lupus-like Disease in MRL/lpr Mice. *Arthritis Rheumatol.* 75, 1395–1406. <https://www.ncbi.nlm.nih.gov/pubmed/36897808>.
- Nickerson, K.M., Smita, S., Hoehn, K.B., Marinov, A.D., Thomas, K.B., Kos, J.T., Yang, Y., Bastacky, S.I., Watson, C.T., Kleinstein, S.H., and Shlomchik, M.J. (2023). Age-associated B cells are heterogeneous and dynamic drivers of autoimmunity in mice. *J. Exp. Med.* 220, e20221346. <https://www.ncbi.nlm.nih.gov/pubmed/36828389>.
- Marinov, A.D., Wang, H., Bastacky, S.I., van Puijenbroek, E., Schindler, T., Speziale, D., Perro, M., Klein, C., Nickerson, K.M., and Shlomchik, M.J. (2021). The Type II Anti-CD20 Antibody Obinutuzumab (GA101) Is More Effective Than Rituximab at Depleting B Cells and Treating Disease in a Murine Lupus Model. *Arthritis Rheumatol.* 73, 826–836. <https://www.ncbi.nlm.nih.gov/pubmed/33277983>.
- Lou, H., Ling, G.S., and Cao, X. (2022). Autoantibodies in systemic lupus erythematosus: From immunopathology to therapeutic target. *J. Autoimmun.* 132, 102861. <https://www.ncbi.nlm.nih.gov/pubmed/35872103>.
- Chan, O.T., Madaio, M.P., and Shlomchik, M.J. (1999). B cells are required for lupus nephritis in the polygenic, Fas-intact MRL model of systemic autoimmunity. *J. Immunol.* 163, 3592–3596. <https://www.ncbi.nlm.nih.gov/pubmed/10490951>.
- Chan, O., Madaio, M.P., and Shlomchik, M.J. (1997). The roles of B cells in MRL/lpr murine lupus. *Ann. N. Y. Acad. Sci.* 815, 75–87. <https://www.ncbi.nlm.nih.gov/pubmed/9186641>.
- Hao, F., Tian, M., Feng, Y., Quan, C., Chen, Y., Chen, S., and Wei, M. (2018). Abrogation of Lupus Nephritis in Somatic Hypermutation-Deficient MRL/lpr Mice. *J. Immunol.* 200, 3905–3912. <https://www.ncbi.nlm.nih.gov/pubmed/29728506>.
- Atisha-Fregoso, Y., Toz, B., and Diamond, B. (2021). Meant to Be: B cells as a therapeutic target in systemic lupus erythematosus. *J. Clin. Invest.* 131, e149095. <https://www.ncbi.nlm.nih.gov/pubmed/34128474>.
- Lee, D.S.W., Rojas, O.L., and Gommerman, J.L. (2021). B cell depletion therapies in autoimmune disease: advances and mechanistic insights. *Nat. Rev. Drug Discov.* 20, 179–199. <https://www.ncbi.nlm.nih.gov/pubmed/33324003>.
- Lu, L.D., Stump, K.L., Wallace, N.H., Dobrzanski, P., Serdikoff, C., Gingrich, D.E., Dugan, B.J., Angeles, T.S., Albom, M.S., Mason, J.L., et al. (2011). Depletion of autoreactive plasma cells and treatment of lupus nephritis in mice using CEP-33779, a novel, orally active, selective inhibitor of JAK2. *J. Immunol.* 187, 3840–3853. <https://www.ncbi.nlm.nih.gov/pubmed/21880982>.
- Hoffman, W., Lakkis, F.G., and Chalasani, G. (2016). B Cells, Antibodies, and More. *Clin. J. Am. Soc. Nephrol.* 11, 137–154. <https://www.ncbi.nlm.nih.gov/pubmed/26700440>.
- Xiao, W., Zhang, Q., Jiang, F., Pins, M., Kozlowski, J.M., and Wang, Z. (2003). Suppression of prostate tumor growth by U19, a novel testosterone-regulated apoptosis inducer. *Cancer Res.* 63, 4698–4704. <https://www.ncbi.nlm.nih.gov/pubmed/12907652>.
- Luo, R.T., Lavau, C., Du, C., Simone, F., Polak, P.E., Kawamata, S., and Thirman, M.J. (2001). The elongation domain of ELL is dispensable but its ELL-associated factor 1 interaction domain is essential for MLL-ELL-induced leukemogenesis. *Mol. Cell Biol.* 21, 5678–5687. <https://www.ncbi.nlm.nih.gov/pubmed/11463848>.
- Simone, F., Luo, R.T., Polak, P.E., Kaberlein, J.J., and Thirman, M.J. (2003). ELL-associated factor 2 (EAF2), a functional homolog of EAF1 with alternative ELL binding properties. *Blood* 101, 2355–2362. <https://www.ncbi.nlm.nih.gov/pubmed/12446457>.
- Simone, F., Polak, P.E., Kaberlein, J.J., Luo, R.T., Levitan, D.A., and Thirman, M.J. (2001). EAF1, a novel ELL-associated factor that is delocalized by expression of the MLL-ELL fusion protein. *Blood* 98, 201–209. <https://www.ncbi.nlm.nih.gov/pubmed/11418481>.
- Kong, S.E., Banks, C.A.S., Shilatfard, A., Conaway, J.W., and Conaway, R.C. (2005). ELL-associated factors 1 and 2 are positive regulators of RNA polymerase II elongation factor ELL. *Proc. Natl. Acad. Sci. USA* 102, 10094–10098. <https://www.ncbi.nlm.nih.gov/pubmed/16006523>.
- Luo, Z., Lin, C., and Shilatfard, A. (2012). The super elongation complex (SEC) family in transcriptional control. *Nat. Rev. Mol. Cell Biol.* 13, 543–547. <https://www.ncbi.nlm.nih.gov/pubmed/22895430>.
- Li, Y., Takahashi, Y., Fujii, S.I., Zhou, Y., Hong, R., Suzuki, A., Tsubata, T., Hase, K., and Wang, J.Y. (2016). EAF2 mediates germinal centre B-cell apoptosis to suppress excessive immune responses and prevent autoimmunity. *Nat. Commun.* 7, 10836. <https://www.ncbi.nlm.nih.gov/pubmed/26935903>.
- Fang, T., Li, B., Li, M., Zhang, Y., Jing, Z., Li, Y., Xue, T., Zhang, Z., Fang, W., Lin, Z., et al. (2023). Engineered Cell Membrane Vesicles Expressing CD40 Alleviate Systemic Lupus Nephritis by Intervening B Cell Activation. *Small Methods* 7, e2200925. <https://www.ncbi.nlm.nih.gov/pubmed/36605001>.
- Wang, Y., Liu, J., Burrows, P.D., and Wang, J.Y. (2020). B Cell Development and Maturation. *Adv. Exp. Med. Biol.* 1254, 1–22. <https://www.ncbi.nlm.nih.gov/pubmed/32323265>.
- Yamamoto, W., Toyoda, H., Xu, D.Q., Hanaki, R., Morimoto, M., Nakato, D., Ito, T., Iwamoto, S., Bonno, M., Tanaka, S., and Hirayama, M. (2018). CD3+ B-1a Cells as a Mediator of Disease Progression in Autoimmune-Prone Mice. *Mediat. Inflamm.* 2018, 9289417. <https://www.ncbi.nlm.nih.gov/pubmed/30670930>.
- Reap, E.A., Sobel, E.S., Cohen, P.L., and Eisenberg, R.A. (1993). Conventional B cells, not B-1 cells, are responsible for producing autoantibodies in lpr mice. *J. Exp. Med.* 177, 69–78. <https://www.ncbi.nlm.nih.gov/pubmed/8418209>.
- Lech, M., Weidenbusch, M., Kulkarni, O.P., Ryu, M., Darisipudi, M.N., Susanti, H.E.,

- Mittrucker, H.W., Mak, T.W., and Anders, H.J. (2011). IRF4 deficiency abrogates lupus nephritis despite enhancing systemic cytokine production. *J. Am. Soc. Nephrol.* 22, 1443–1452. <https://www.ncbi.nlm.nih.gov/pubmed/21742731>.
31. Li, H., and Tsokos, G.C. (2021). Double-negative T cells in autoimmune diseases. *Curr. Opin. Rheumatol.* 33, 163–172. <https://www.ncbi.nlm.nih.gov/pubmed/33394752>.
32. Velikkakam, T., Gollob, K.J., and Dutra, W.O. (2022). Double-negative T cells: Setting the stage for disease control or progression. *Immunology* 165, 371–385. <https://www.ncbi.nlm.nih.gov/pubmed/34939192>.
33. Wu, Z., Zheng, Y., Sheng, J., Han, Y., Yang, Y., Pan, H., and Yao, J. (2022). CD3(+)/CD4(-)/CD8(-) (Double-Negative) T Cells in Inflammation, Immune Disorders and Cancer. *Front. Immunol.* 13, 816005. <https://www.ncbi.nlm.nih.gov/pubmed/35222392>.
34. Chan, O.T., Hannum, L.G., Haberman, A.M., Madaio, M.P., and Shlomchik, M.J. (1999). A novel mouse with B cells but lacking serum antibody reveals an antibody-independent role for B cells in murine lupus. *J. Exp. Med.* 189, 1639–1648. <https://www.ncbi.nlm.nih.gov/pubmed/10330443>.
35. Chan, O.T., Madaio, M.P., and Shlomchik, M.J. (1999). The central and multiple roles of B cells in lupus pathogenesis. *Immunol. Rev.* 169, 107–121. <https://www.ncbi.nlm.nih.gov/pubmed/10450512>.
36. Akashi, T., Nagafuchi, S., Anzai, K., Kitamura, D., Wang, J., Taniuchi, I., Niho, Y., and Watanabe, T. (1998). Proliferation of CD3+ B220- single-positive normal T cells was suppressed in B-cell-deficient lpr mice. *Immunology* 93, 238–248. <https://www.ncbi.nlm.nih.gov/pubmed/9616374>.
37. Hao, Z., Duncan, G.S., Seagal, J., Su, Y.W., Hong, C., Haight, J., Chen, N.J., Elia, A., Wakeham, A., Li, W.Y., et al. (2008). Fas receptor expression in germinal-center B cells is essential for T and B lymphocyte homeostasis. *Immunity* 29, 615–627. <https://www.ncbi.nlm.nih.gov/pubmed/18835195>.
38. Li, Y., Ding, T., Chen, J., Ji, J., Wang, W., Ding, B., Ge, W., Fan, Y., and Xu, L. (2022). The protective capability of Hedyotis diffusa Willd on lupus nephritis by attenuating the IL-17 expression in MRL/lpr mice. *Front. Immunol.* 13, 943827. <https://www.ncbi.nlm.nih.gov/pubmed/35958622>.
39. Anders, H.J., Saxena, R., Zhao, M.H., Parodis, I., Salmon, J.E., and Mohan, C. (2020). Lupus nephritis. *Nat. Rev. Dis. Prim.* 6, 7. <https://www.ncbi.nlm.nih.gov/pubmed/31974366>.
40. Andrews, B.S., Eisenberg, R.A., Theofilopoulos, A.N., Izui, S., Wilson, C.B., McConahey, P.J., Murphy, E.D., Roths, J.B., and Dixon, F.J. (1978). Spontaneous murine lupus-like syndromes. Clinical and immunopathological manifestations in several strains. *J. Exp. Med.* 148, 1198–1215. <https://www.ncbi.nlm.nih.gov/pubmed/309911>.
41. Elshikha, A.S., Lu, Y., Chen, M.J., Akbar, M., Zeumer, L., Ritter, A., Elghamry, H., Mahdi, M.A., Morel, L., and Song, S. (2016). Alpha 1 Antitrypsin Inhibits Dendritic Cell Activation and Attenuates Nephritis in a Mouse Model of Lupus. *PLoS One* 11, e0156583. <https://www.ncbi.nlm.nih.gov/pubmed/27232337>.
42. Green, D.R., Droin, N., and Pinkoski, M. (2003). Activation-induced cell death in T cells. *Immunol. Rev.* 193, 70–81. <https://www.ncbi.nlm.nih.gov/pubmed/12752672>.
43. Arakaki, R., Yamada, A., Kudo, Y., Hayashi, Y., and Ishimaru, N. (2014). Mechanism of activation-induced cell death of T cells and regulation of FasL expression. *Crit. Rev. Immunol.* 34, 301–314. <https://www.ncbi.nlm.nih.gov/pubmed/24941158>.
44. Tsokos, G.C. (2011). Systemic lupus erythematosus. *N. Engl. J. Med.* 365, 2110–2121. <https://www.ncbi.nlm.nih.gov/pubmed/22129255>.
45. Moore, E., and Putterman, C. (2020). Are lupus animal models useful for understanding and developing new therapies for human SLE? *J. Autoimmun.* 112, 102490. <https://www.ncbi.nlm.nih.gov/pubmed/32535128>.
46. Chen, Y., Chen, Y., Shi, C., Huang, Z., Zhang, Y., Li, S., Li, Y., Ye, J., Yu, C., Li, Z., et al. (2018). SOAPnuke: a MapReduce acceleration-supported software for integrated quality control and preprocessing of high-throughput sequencing data. *GigaScience* 7, 1–6. <https://www.ncbi.nlm.nih.gov/pubmed/29220494>.
47. Kim, D., Langmead, B., and Salzberg, S.L. (2015). HISAT: a fast spliced aligner with low memory requirements. *Nat. Methods* 12, 357–360. <https://www.ncbi.nlm.nih.gov/pubmed/25751142>.
48. Langmead, B., and Salzberg, S.L. (2012). Fast gapped-read alignment with Bowtie 2. *Nat. Methods* 9, 357–359. <https://www.ncbi.nlm.nih.gov/pubmed/22388286>.
49. Li, B., and Dewey, C.N. (2011). RSEM: accurate transcript quantification from RNA-Seq data with or without a reference genome. *BMC Bioinf.* 12, 323. <https://www.ncbi.nlm.nih.gov/pubmed/21816040>.
50. Qian, Y., Conway, K.L., Lu, X., Seitz, H.M., Matsushima, G.K., and Clarke, S.H. (2006). Autoreactive MZ and B-1 B-cell activation by FasLpr is coincident with an increased frequency of apoptotic lymphocytes and a defect in macrophage clearance. *Blood* 108, 974–982. <https://www.ncbi.nlm.nih.gov/pubmed/16861350>.
51. Jarad, G., Lakhe-Reddy, S., Blatnik, J., Koepke, M., Khan, S., El-Deanawy, M.A., O'Connor, A.S., Sedor, J.R., and Schelling, J.R. (2004). Renal phenotype is exacerbated in Os and lpr double mutant mice. *Kidney Int.* 66, 1029–1035. <https://www.ncbi.nlm.nih.gov/pubmed/15327396>.
52. Lai, N., Min, Q., Xiong, E., Liu, J., Zhang, L., Yasuda, S., and Wang, J.Y. (2019). A tetrameric form of CD40 ligand with potent biological activities in both mouse and human primary B cells. *Mol. Immunol.* 105, 173–180. <https://www.ncbi.nlm.nih.gov/pubmed/30529036>.

STAR★METHODS

KEY RESOURCES TABLE

REAGENT or RESOURCE	SOURCE	IDENTIFIER
Antibodies		
Alexa Fluor 488 goat anti-mouse IgG (H + L)	Invitrogen	Cat#A28175; RRID: AB_2536161
HRP-conjugated anti-mouse IgG (H + L)	Southern Biotech	Cat#1030-05; RRID: AB_2619742
Anti-mouse Ig antibody	Southern Biotech	Cat#1010-01; RRID: AB_2794121
HRP-conjugated anti-mouse IgM	Southern Biotech	Cat#1020-05; RRID: AB_2794201
HRP-conjugated anti-mouse IgA	Southern Biotech	Cat#1040-05; RRID: AB_2714213
Purified Rat Anti-Mouse CD16/CD32	BD Biosciences	Cat#553142; RRID: AB_394656
FITC-conjugated anti-mouse -CD43	BD Biosciences	Cat#553270; RRID: AB_394747
APC-conjugated anti-mouse -CD5	Biolegend	Cat#100626; RRID: AB_2563929
APC-Cy7-conjugated anti-mouse B220	BD Biosciences	Cat#552094; RRID: AB_394335
PE-Cyaine 7-conjugated anti-mouse B220	Biolegend	Cat#103222; RRID: AB_313005
Percp Cy5.5-conjugated anti-mouse B220	Biolegend	Cat#103235; RRID: AB_893356
APC-conjugated anti-mouse -CD93	eBioscience	Cat#17-5892-81; RRID: AB_469465
PE-Cyaine 7-conjugated anti-mouse -CD23	Biolegend	Cat#101614; RRID: AB_2103036
FITC-conjugated anti-mouse -CD21/35	BD Biosciences	Cat#553818; RRID: AB_395070
APC-conjugated anti-mouse -CD69	BD Biosciences	Cat#560689; RRID: AB_1727506
APC-conjugated anti-mouse -CD86	Invitrogen	Cat#17-0862-82; RRID: AB_469419
FITC-conjugated anti-mouse -GL-7	Biolegend	Cat#144604; RRID: AB_2561697
PE- conjugated anti-mouse -CD138	BD Biosciences	Cat#553714; RRID: AB_395000
APC- conjugated anti-mouse -CD138	BD Biosciences	Cat#558626; RRID: AB_1645216
APC-Cy7-conjugated anti-mouse -CD3	Biolegend	Cat#152323; RRID: AB_2894632
APC- conjugated anti-mouse -CD3	Biolegend	Cat#100235; RRID: AB_2561455
APC- conjugated anti-mouse -CD4	Biolegend	Cat#100412; RRID: AB_312697
PE-Cyaine 7-conjugated anti-mouse -CD8	Biolegend	Cat#140416; RRID: AB_2564385
7-amino-actinomycin D	Invitrogen	Cat#00-6993-50
APC- conjugated Annexin-V	BD Biosciences	Cat#550474; RRID: AB_2868885
FITC- conjugated Annexin-V	BD Biosciences	Cat#556420; RRID: AB_2665412
AP-conjugated anti-mouse IgG (H + L)	Southern Biotech	Cat#1031-04; RRID: AB_2794306
AP-conjugated anti-mouse IgM	Southern Biotech	Cat#1021-04; RRID: AB_2794239
F(ab') ₂ anti-mouse μ chain-specific antibodies	Jackson ImmunoResearch	Cat#715-006-020; RRID: AB_2340760
Chemicals, peptides, and recombinant proteins		
Mouse IL-4	R&D	Cat#404-ML
Mouse IL-21	R&D	Cat#594-ML
Annexin-V Binding buffer	Biolegend	Cat#422201
Lipopolysaccharide	Sigma	Cat#437627
CD40 ligand	This paper	N/A
Critical commercial assays		
Urine protein quantification test kit	Nanjing Jiancheng Bioengineering institute	Cat#C035-2-1
Mouse B Lymphocyte Enrichment Set-DM	BD Biosciences	Cat#557792
BCIP/NBT substrate	Beyotime	Cat#C3206

(Continued on next page)

Continued

REAGENT or RESOURCE	SOURCE	IDENTIFIER
Mouse ANA ELISA kit	Creative Diagnostics	Cat#DEIA-BJ2332
Deposited data		
RNA-seq data	GEO	Accession numbers : GSE278963
Experimental models: Organisms/strains		
MRL/lpr female mice	Jackson Laboratory	N/A
<i>Eaf2</i> ^{-/-} mice	Li et al. ²⁵	N/A
Software and algorithms		
GraphPad Prism	GraphPad	https://www.graphpad.com/
ImageJ	NIH	https://imagej.nih.gov/ij/
FlowJo	BD Biosciences	https://www.flowjo.com/
SOAPnuke (v1.6.5)	Chen et al. ⁴⁶	https://github.com/BGI-flexlab/SOAPnuke
HISAT (v2.2.1)	Kim et al. ⁴⁷	http://www.ccb.jhu.edu/software/hisat
Bowtie2 (v2.4.5)	Langmead et al. ⁴⁸	http://bowtie-bio.sourceforge.net/Bowtie2/index.shtml
RSEM (v1.3.1)	Li et al. ⁴⁹	http://deweylab.biostat.wisc.edu/rsem/rsem-calculate-expression.html

EXPERIMENTAL MODEL AND STUDY PARTICIPANT DETAILS**Mouse model**

MRL/lpr mice were purchased from the Jackson Laboratory (Bar Harbor, ME). *Eaf2*^{-/-} mice, previously generated,²⁵ were crossed with MRL/lpr mice to produce F1 offspring.⁵⁰ These F1 mice carrying the *Eaf2*^{+/-}*Fas*^{+/lpr} genotype underwent brother-sister mating to generate F2 mice⁵¹ with various genotypes including WT, *Eaf2*^{-/-}, *Fas*^{lpr/lpr} (hereafter *Fas*^{lpr}), and *Eaf2*^{-/-}*Fas*^{lpr} on a mixed genetic background. F2 siblings were further mated to obtain a sufficient number of mice with various genotypes. The *Eaf2* genotype was determined using previously described methods [25], and the *lpr* genotype was identified by genomic PCR of tail DNA following the vendor's protocol. Twenty-four mouse tails from the initial cohort and from a subsequent one-year interval were sent to Shanghai Biowing Applied Biotechnology for genomic single nucleotide polymorphism (SNP) testing, confirming comparable genetic backgrounds across the four genotypes (Figure S1). Only female mice aged 7 to 25 weeks were used for phenotypic and functional analyses. All mice were housed under specific pathogen-free conditions at the Laboratory Animal Facility of Fudan University, with a standard diet and a 12-h light-dark cycle, maintained at controlled temperature and humidity. All animal procedures were approved by the Animal Experimentation Committee of Fudan University.

METHOD DETAILS**Evaluation of renal injury**

Urine samples were collected biweekly from individual mice using the 'bladder massage' approach, and urine protein (UP) concentrations were measured at 17 weeks with a urine protein quantification test kit (C035-2-1, Nanjing Jiancheng Bioengineering institute). Serum blood urea nitrogen (BUN) levels were assessed at 17 weeks using a fully automated biochemical analyzer at the Laboratory Animal Facility of Fudan University. Kidneys were fixed in 4% polyformaldehyde, embedded in paraffin, and sectioned for staining with hematoxylin and eosin (H&E) and periodic acid-Schiff (PAS). Glomeruli areas and numbers were measured with ImageJ software. Immunofluorescence staining for immune complex deposition in kidneys was performed on 4- μ m paraffin sections using Alexa Fluor 488 goat anti-mouse IgG antibody (A28175, Invitrogen).

ELISA

Sera collected at 17 weeks were analyzed for antibodies and autoantibodies using an enzyme-linked immunosorbent assay (ELISA). Plates were coated with 1 μ g/mL sm/RNP and incubated overnight at 4°C. Samples or standards were added, followed by HRP-conjugated anti-mouse IgG (H + L) antibody (1030-05, Southern Biotech). For IgG anti-ssDNA detection, 10 μ g/ml calf thymus DNA was denatured before coating the plates, left at room temperature for 1 h, and processed as described above. ANA levels were measured using a mouse ANA ELISA kit (DEIA-BJ2332, Creative Diagnostics) according to the manufacturer's protocol. To analyze IgG, IgM, IgA concentrations in serum and culture supernatants of mouse splenic B cells, anti-mouse Ig antibody (1010-01, Southern Biotech) was used as the primary antibody, followed by HRP-conjugated secondary antibodies specific for IgG (H + L), IgM (1020-05, Southern Biotech), and IgA (1040-05, Southern Biotech).

Flow cytometry

Single-cell suspensions were incubated with anti-CD16/32 (2.4G2, 553142; BD Biosciences) to block Fc γ R, and then stained with the following fluorochrome-conjugated Abs including α -CD43(553270, BD Biosciences), α -CD5 (100626, Biolegend), α -B220 (552094, BD Biosciences; 103222, 103235, Biolegend), α -CD93 (17-5892-81, eBioscience), α -IgM (553408, BD Biosciences), α -CD23 (101614, Biolegend), α -CD21/35 (553818, BD Biosciences), α -CD69 (560689, BD Biosciences), α -CD86 (17-0862-82, Invitrogen), α -GL-7 (144604, Biolegend), α -CD138 (558626, 553714, BD Biosciences), α -CD3 (152323, 100235, Biolegend), α -CD4 (100412, Biolegend), and α -CD8 (140416, Biolegend). 7-amino-actinomycin D (7-AAD, Invitrogen, 00-6993-50) was used to distinguish live from dead cells. Samples were analyzed on a FACS^{Verse} flow cytometer (BD Biosciences), and data were processed using FlowJo software (Tree Star, Ashland, OR, USA).

Apoptosis assay

Single cell suspensions were first stained for surface markers, washed twice with Binding buffer (422201, Biolegend), and then stained with Annexin-V (550474, BD Biosciences, 1:100) and 7-AAD (1:100) on ice for 15 min. Samples were analyzed using a FACS^{Verse} flow cytometer (BD Biosciences), and data were processed using FlowJo software.

B cell purification and ex vivo stimulation

B cells were isolated using the Mouse B Lymphocyte Enrichment Set-DM (BD Biosciences) via magnetic bead negative selection. Briefly, splenic single-cell suspensions from mice aged 7–12 weeks were mixed with Biotinylated Mouse B Lymphocyte Enrichment Cocktail. After washing, IMag Streptavidin Particles Plus were added to the cell suspension, and the bound cells were separated using a magnetic stand. The purity of the cell population was confirmed by flow cytometry to be >90%. Purified B cells were stimulated with Lipopolysaccharide (LPS) (Sigma, 20 μ g/mL), CD40 ligand (CD40L) (house made, 0.1V)⁵² + IL4 (R&D, 20 ng/mL) + IL21 (R&D, 30 ng/mL) (CLL), or F(ab')₂ anti-mouse μ chain-specific antibodies (Jackson ImmunoResearch, 10 μ g/mL) + CD40L + IL4 (ACI), and cultured in 96-well U plates for 24 and 72 h to analyze cell activation and differentiation.

ELISPOT assay

The PVDF membrane of an ELISPOT plate was activated with 70% ethanol, coated with anti-mouse Ig antibody overnight at 4°C, and blocked for 2 h. LPS- or CII-stimulated cells were added to wells and incubated for 4 h at 37°C in a cell culture incubator. AP-conjugated secondary antibodies (anti-mouse IgG, 1031-04; anti-mouse IgM, 1021-04; SouthernBiotech) and BCIP/NBT substrate (C3206, Beyotime) were applied for detection. Data were acquired using an enzyme-linked spot analyzer, iSpot.

RNA sequencing (RNA-seq)

B220⁺CD3⁺ cells were sorted from *Fas*^{lpr} and *Eaf2*^{-/-}*Fas*^{lpr} mice for RNA-Seq at BGI Genomics. The raw data was filtered with SOAPnuke⁴⁶ (v1.6.5, <https://github.com/BGI-flexlab/SOAPnuke>) to obtain clean reads stored in FASTQ format. The clean data was mapped to the reference genome by HISAT⁴⁷ (v2.2.1, <http://www.ccb.jhu.edu/software/hisat>). The clean data was mapped to the assembled specific gene by Bowtie2⁴⁸ (v2.4.5, <http://bowtie-bio.sourceforge.net/Bowtie2/index.shtml>). The expression level of genes was calculated by RSEM⁴⁹ (v1.3.1, <http://deweylab.biostat.wisc.edu/rsem/rsem-calculate-expression.html>). The subsequent analysis and data mining were performed on Dr. Tom Multi-omics Data mining system (<https://biosys.bgi.com>) except for the volcano plot, which was depicted using an online platform for data analysis and visualization (<https://www.bioinformatics.com.cn>).

QUANTIFICATION AND STATISTICAL ANALYSIS

Statistical analyses were conducted using GraphPad Prism version 8.4.2 software. Two-tailed unpaired and paired Student's t-tests were used to assess differences between two groups or time points, respectively. One-way and two-way ANOVA were used to test effects among multiple groups. Log rank test was used to analyze survival data in mice. *p*-values <0.05 were considered to be statistically significant, represented as **p* < 0.05, ***p* < 0.01, ****p* < 0.001, *****p* < 0.0001. Data are represented as mean \pm SEM, except for the body weight and survival curves.